Aalto University

Cerna, Fernando V.; Pourakbari Kasmaei, Mahdi; Lehtonen, Matti; Contreras, Javier

Efficient Automation of an HEV Heterogeneous Fleet using a Two-Stage Methodology

Please cite the original version:
Cerna, F. V., Pourakbari Kasmaei, M., Lehtonen, M., & Contreras, J. (2019). Efficient Automation of an HEV Heterogeneous Fleet using a Two-Stage Methodology. *IEEE Transactions on Vehicular Technology*, *68*(10), 9494-9506. https://doi.org/10.1109/TVT.2019.2937452

Efficient Automation of an HEV Heterogeneous Fleet using a Two-Stage Methodology

Fernando V. Cerna, Mahdi Pourakbari-Kasmaei, *Member, IEEE*, Matti Lehtonen, and Javier Contreras, *Fellow, IEEE*

Abstract—An influential factor in enhancing the attendance services, mainly in commercial and emergency sectors, is the vehicular technology used to transport people, goods, or equipment. Although hybrid electric vehicles (HEVs) represent a sustainable transport alternative, the existing technical limitations such as battery and fuel capacities, and autonomy, among others, highlight the provision of an efficient automation tool. The tool can serve to enhance the operational performance of the HEV by selecting the proper driving mode (on fuel or electricity), and the navigation strategies to the delivery and charging points in urban areas. This paper proposes a two-stage methodology that allows the HEVs operators to automate the operational performance of a heterogeneous HEV fleet on a city map. Each stage is handled by its corresponding optimization model. In the first stage, the total navigation time and the battery lifetime of the fleet during the operation are optimized. In this stage, constraints related to charge-sustaining/charge-depleting modes, state of charge (SoC) of the HEVs battery, and deliveries schedules are taken into account. To this end, operating strategies related to the performance of different types of existing HEV technologies are anonymously considered. In the second stage, the best operating strategy among all the operating strategies is selected while considering the capacity of HEVs to deliver a given quantity of goods. Moreover, uncertainties during the HEV navigation are simulated considering the change in traffic density of the urban roads as a function of the levels of service (LOS). Results show that the proposed methodology establishes an efficient operational scheme for a HEVs fleet, ensuring a significant reduction of energy usage as well as mitigating the CO_2 emissions.

Index Terms—Attendance services, Battery charging, HEV heterogeneous fleet, operating strategies.

NOMENCLATURE

A. Sets and indexes

$k/i,d,e,u$ Indexes stand for intersections i/k, delivery, HEV technology, and density value, respectively.

op/ps Indexed of operation, and operating strategy

Ω_{ur}, Ω_i Set of urban roads ki and intersections i of roads.

Ω_d, Ω_e Set of deliveries points d and HEV technologies e.

Ω_{op}, Ω_{ps} Set of operations s and operating strategies v.

Ω_D Set of density values u.

B. Parameters

au_e Autonomy value of HEV e (km).

b Linear battery degradation cost-intercept parameter.

B_e Battery capacity of the HEV e (kWh).

B^L Battery lifetime in years.

C_e^{HEV} Capacity of HEV e (quantity of goods that can be transported by HEV e).

C^B Battery cost ($/kWh).

C^F Capacity fade at end of life.

l_{ki}, D_{ki} Length of road ki (km), and the corresponding traffic density (veh/km).

D_u Value of the traffic density of element u (veh/km).

D_J Saturation density value (veh/km).

D_0 Optimal density value related to F_{max} (veh/km).

$E_e^{CO_2}$ CO_2 emissions of HEV e (gCO2/km).

F_{max} Maximum traffic flow value (veh/h).

F_{max}^{mr} Maximum traffic flow value on main roads (veh/h).

F_{max}^{sr} Maximum traffic flow value on secondary roads (veh/h).

K^C Fuel capacity (L).

m Linear battery degradation cost-slope parameter.

M Big value used as part of the constraints linearized.

$M_{e,s,v,d}^{del}$ Hyper-matrix related to the deliveries d in operating strategy v of the operation s to be performed by HEV e.

$M_{e,s,v}^{fob}$ Hyper-matrix related to the objective function values of operating strategy v for operation s of HEV e.

N^d Total number of points to be visited (delivery points and warehouse).

P_e^{ch} Charging rate of HEV e (kW).

$P_u^{mr/sr}$ Probability values related to D_u at main/secondary roads, respectively.

$P_u^{amr/asr}$ Accumulated probability value related to P_u^{mr} or P_u^{sr}.

r_i^s Type of intersection i (1: if the intersections has a charging station, otherwise 0).

SOC_e^o Initial SoC of the battery of HEV e (kWh).

$t_{d,i}^n$ Indicates the type of intersection i at delivery d.

t_{ki}^{ur} Indicates the type of road ki (1: main; 0: secondary).

U_s^{op} Quantity of goods to be demanded in operation s.

v_{ki} Maximum average speed value of road ki (km/h).

v_f Free flow speed value (km/h).

v_0 Optimal speed value related to F_{max} (km/h).

v_0^{mr}/v_0^{sr} Optimal speed related to F_{max}^{mr} or F_{max}^{sr} (km/h).

δ^{nt}, δ^{bl} Weighted weights related to total navigation time, and battery lifetime.

δ^{ue} Extra units cost ($/units).

β Parameter for defining the nodes status of $t_{d,i}^n$ (-1: starting node; 0: intermediate node; 1: arrival node).

δ_e^C Fuel consumption rate (km/L).

ρ^C Percentage of CO_2 emissions reduction.

F. V. Cerna is with the Department of Electrical Engineering, Federal University of Roraima (UFRR), Av. Cap. Ene Garcês, n° 2413 - Aeroporto, Boa Vista - RR, 69310-000 (e-mail: fvcerna83@gmail.com).

Mahdi Pourakbari-Kasmaei, and Matti Lehtonen are with the Department of Electrical Engineering and Automation, Aalto University, Maarintie 8, 02150, Espoo, Finland (e-mails: Mahdi.Pourakbari@aalto.fi, Matti.Lehtonen}@aalto.fi).

Javier Contreras is with the E.T.S. de Ingenieros Industriales, University of Castilla–La Mancha, 13071 Ciudad Real, Spain (e-mail: Javier.Contreras@uclm.es).

δ_e^{PE} Percentage of battery capacity, used to calculate the SoC of HEV e returning to the warehouse.

δ_e^D Rate of energy spend by HEV e (kWh/km).

$[\overline{\tau}^{ch}, \underline{\tau}^{ch}]$ Charging time variation interval (h).

η^{cE}/η^{dE} Charging/discharging efficiencies values.

C. Variables

$\omega_{e,d,ki}$ Decides the travel of HEV e in road ki for delivery d.

$l_{e,d,ki}^{CSM/CDM}$ Length of road ki that HEV e travels in CSM/CDM for delivery d.

$SOC_{e,d,i}$ SoC of the battery of HEV e at the intersection i, at delivery d (kWh).

$SOC_{e,d,i}^a$ SoC of the battery of HEV e when arrives at the intersection i at delivery d (kWh).

$\varepsilon_{e,d,i}$ Energy for charging of HEV e at intersection i for delivery d (kWh).

$\tau_{e,d,i}^{ch}$ Denotes the charging time of HEV e at charging station located in the intersection i during delivery d (h).

$y_{e,d,i}$ Stands for the charging status of HEV e at intersection i during delivery d.

$\Delta\omega_{e,d,ki}^{CDM}$ Represents the product of $\omega_{e,d,ki}$ and $l_{e,d,ki}^{CDM}$ at the linearized constraints.

$\Delta'_{e,d,ki}$ Represents the product of $\omega_{e,d,ki}$ and $SOC_{e,d,k}$ at the linearized constraints.

$\Delta\tau_{e,d,i}^{ch}$ Represents the product of $y_{e,d,i}$ and $\tau_{e,d,i}^{ch}$ at the linearized constraints.

$Z_{e,s,v}$ Decides which operation s is made by HEV e via the operating strategy v.

ΔC^{HEV} Total extra quantity of goods.

I. INTRODUCTION

THE electricity demand by the transportation sector will increase sharply after 2020 due to the projected increase in sales of new electric vehicles (EVs) and hybrid electric vehicles (HEVs) [1]. In this context, service sectors, mainly commercial (e.g., postal, merchandise, home care, etc.) and emergency (e.g., ambulances, fire engines, police vehicles, energy company cars, etc.), can have a positive influence, since the quality of their attendance depends largely on the vehicular technologies used to transport people, goods and/or equipment in urban areas [2]. These services present several challenges such as minimizing delay times, managing fuel consumption, selecting the most appropriate route, etc., thereby affecting the vehicle fleet performance. These challenges highlight the crucial role of electric vehicles and the operational and sustainable aspects to be considered within an efficient automation strategy during their operation [3], [4].

Studies show that among EV-based technologies, the HEV is a promising alternative in the transportation sector, mostly due to socio-environmental factors [5], [6]. Basically, HEVs present two driving modes during navigation such as 1) Charge-Sustaining Mode (CSM), and 2) Charge-Depleting Mode (CDM). In CSM, the internal combustion engine drives the HEV, whereas, in CDM, the electric energy of the battery is used for driving purposes [7], [8]. If a fleet of HEVs is used to transport goods, their capacity and performance are determining factors that must also be considered in the automation of this particular type of service. Therefore, depending on the quantity of goods, location of supply points and scheduling of operations, proper technology should be assigned. This reveals the significant role of smart tools that

ensure the efficient automation of an HEV heterogeneous fleet considering the optimal CSM/CDM selection, optimal battery management, optimal deliveries scheduling, and environmental issues. Also, the uncertainties due to the variation in traffic density for each road on the urban map, as well as speed limits on roads and sustainable performance of HEVs should be considered in the automation tool [9], [10].

In the literature, most of the existing works related to HEV fleets merely consider the optimal charging or fuel consumption management. In [6], to fulfill the economic criteria of autonomous EVs charging in a city with a predefined spatial limit, a Monte Carlo simulation-based approach was proposed. A mixed-integer linear programming (MILP) model was developed in [11] to coordinate the charging and power storage in the battery of the HEV fleet. In order to optimize the charging profile in the predefined charging points, an energy management system for EV fleet operators was proposed in [12]. In [13], a sensitivity analysis has been done to find the optimal charging process of the EV fleet and the flow exchange between the power grid and EVs. In [14], optimal recharging of EVs considering the different habits of owners was a part of a smart microgrid project in order to manage energy usage, fuel costs, and carbon dioxide emissions, while, as a storage device, addressing the fluctuations of renewable energy output. In [15], a predictive management system was proposed for optimal charging of the HEVs fleets while the charging station was equipped with PVs taken into account the distribution network restrictions. Decentralized control strategies and mathematical programming models for the charging of an EV fleet were developed in [16] and [17]. In [18], an adjustable robust optimization model considering a set of charging stations, travel costs, and battery capacities was investigated. In [19], [20], aiming at minimizing the charging costs, proper policies and charging strategies to determine the optimal scheduling considering historical data were developed. To fairly address the optimal scheduling of EVs, the economic charging and battery degradation were co-optimized in [21] via the Pareto front technique. The EV charging rates were modeled via partial differential equations under three conditions: *1)* EVs receive energy from the grid, *2)* EVs are connected to the grid but not charging, and *3)* EVs deliver energy to the grid, was considered in [22]. Optimal charging scheduling of taxi fleets was presented in [23] while taking into account the charging station locations, unpredictability and balancing issues. Although the aforementioned works highlight the importance of EV charging scheduling, energy management of both EV fleets and charging points and their impact on the electricity grid, both the route as well as the uncertainties involved during navigation of each EV were not part of their focus, while the navigation modes, emissions reduction during navigation, and the EV type (heterogeneous fleet) were also neglected.

In order to fill the aforementioned existing gaps, the performance of EVs and HEVs has been investigated in some works. The integration of thermal power generation units as a support system for PHEV charging has been studied in [24] aiming at minimizing the emissions, especially during peak demand periods. A comparative study on the fuel consumption and emission output of conventional HEVs and plug-in HEVs

were conducted in [25] while taking into account the interaction between the energy storage system, electric machine, power control unit and internal combustion engine. An energy management and vehicle control models were proposed in [26] to simultaneously reduce the fuel consumption and polluting emissions of the HEVs by taking into account the information related to a city road network. In [27], a neural network-based dynamic online programming strategy was used to minimize the fuel consumption of PHEVs where the real-time information, i.e., traffic and control signal, was interchanged between the vehicles and the control center. A management strategy based on the performance of Toyota Prius was investigated in [28] to control the pollutant effects of CO_2 emissions. Internal power flow and its efficient management in the HEV powertrain were analyzed in [29] and [30]. In [29], the limits of the power grid and the waiting and charging times by HEV were considered, while in [30], travel speed, energy level, and stop-and-go frequency were addressed. However, still, there is a lack of smart tools for an effective route and delivery schedule to manage the costs and emissions more effectively.

Investigations related to the determination of the optimal routes, deliveries, and transport capacity of vehicle fleets were addressed in a few works. A mixed-integer quadratically constrained programming (MIQCP) model was proposed in [31] aimed at minimizing the fuel and the recharging costs of the EV fleet in urban areas. However, in this MIQCP model, the traffic density on the main and secondary roads, the direction of the roads, which can be one- or two-way in real-world urban areas, as well as the autonomy of EVs were disregarded. Such oversimplification results in an impractical and unrealistic outcome. In [32], a mathematical formulation for the service network design of a heterogeneous fleet was developed. This formulation considered a set of delivery points with predefined demand and the required time in the scheduling process to reveal the importance of considering a heterogeneous fleet as part of a service network. However, this paper did not take into account the attendance sequences, route types in the transportation network, and aspects related to the sustainable operation of the fleet, i.e., the presence of BEVs, HEVs, or PHEVs. In [33], a mixed-integer linear programming (MILP) model was proposed to solve the vehicle routing problem of the heterogeneous fleet while minimizing the total transportation costs considering a set of vehicles with their transport capacity attending a limited number of customers. A combined energy management strategy, i.e., electricity and fuel consumption, based on frequent route data was developed in [34]. The model considered a set of HEVs and the information related to global positioning and routes while disregarding the location of charging stations and operational characteristics such as navigation time and within urban areas. In [35], to satisfy the transport demand in a given geographical area, a MIQCP model was proposed to guarantee the minimum distance of a fleet of EVs. Although a pure battery fleet represents nearly-zero emissions, its optimal performance is questionable due to the battery charging times and lack of flexibility. In the aforementioned works, the problem of optimal routing considering the transport capacity of vehicular fleets was addressed. However, studies involving the environmental issue

and the use of EVs/HEVs heterogeneous fleet as sustainable forms of transport in the service sector are scarce in the literature.

Works related to EVs and HEVs considering charging batteries and navigation routes for deliveries were developed in [7], [8], [36]. It is worth mentioning that the main motivation of our proposed model is to fill the existing gaps in these works. The authors in [7] and [8] addressed the performance of HEVs during navigation taking into account the driving modes. In [7], the automation of HEVs driving modes within an urban area was addressed via an MILP model taking into account traffic density variations in main and secondary urban roads. In [8], the trip information, charging stations along with path planning, were considered to minimize the fuel consumption by selecting the most appropriate driving mode. The model was handled by dynamic programming for offline mode, while a novel algorithm, namely *online*, was used for real-time optimization purposes. In [36], the optimal operation of a fleet of EVs was guaranteed via a MILP model considering a predefined number of deliveries to be made within a city map. In this model, the shortest distances and minimum operating times of the EVs for each delivery was targeted. However, due to long battery charging times in purely battery-based EVs, it represents an operational limitation in the commercial service and emergency sectors. In contrast, HEVs that have different driving modes represent a more promising alternative in these sectors. To this end, four HEV technologies were tested in [37] via a MILP model that aims to optimize maintenance costs while guaranteeing the CO_2 emission reduction. In this work, the performance of each HEV belonging to the fleet was evaluated individually by the proposed model. In these approaches, the transport capacities of the EVs and HEVs, as well as the selection of the best operating strategy, were not considered.

Consequently, in order to fill the aforementioned existing gaps, this paper proposes a two-stage methodology for the efficient automation of an HEV heterogeneous fleet that enables the service operators to ensure the optimal operational strategy of the vehicle fleet during deliveries. In the first stage, all the operating strategies related to the performance of each type of HEV are determined taking into account the optimal selection of CSM and CDM, as well as a set of constraints related to CO_2 emissions level, SoC of HEVs and deliveries scheduling aiming at minimizing the maintenance and overtime costs. In the second stage, the best operating strategy for a type of HEV technology considering constraints related to the goods supply capacity is obtained. Uncertainties, due to traffic density variation in the operation of HEV, are modeled considering the probability values corresponds to the levels of service (LOS). The model of the urban map presents a graph with 412 nodes (intersections between main and secondary roads) and 832 roads. In order to obtain more realistic results of the HEV heterogeneous fleet during operation on the urban map, real-data of the existing HEVs technology are anonymously used. Our work goes beyond the models proposed in [7], [36], and [37]. In [7] and [37], investigations related to the performance of HEV technologies were carried out and in [36] the management of a homogeneous fleet of EVs was developed. These technologies have less robust batteries and different
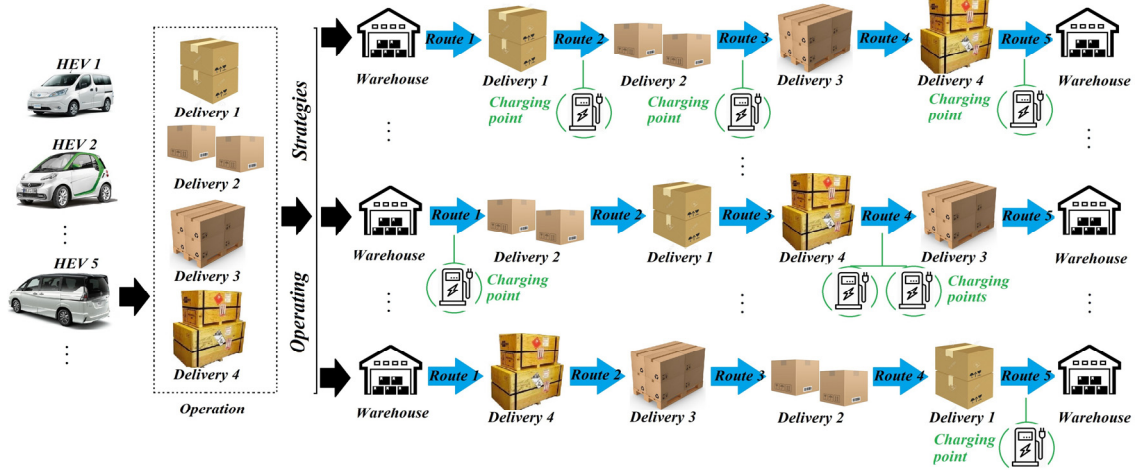
Fig. 2. Possible sequences for the delivery of product (operating strategies) related to a given operation.
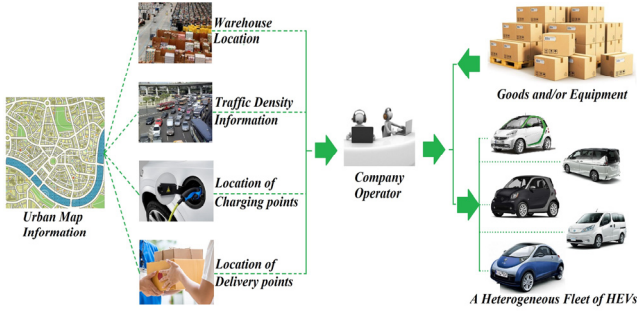

Fig. 1. Operational diagram of a service company.

modes of navigation, thus allowing to optimize the delivery and charging time during the operation of HEV. The proposed approach ensures the efficient automation of the HEV heterogeneous fleet during the navigation considering CO_2 emissions reduction, and the goods supply capacities associated with the type of HEV technology. In order to find the optimal solution, the AMPL [48] software is used for implementation purpose while the model is solved via the commercial solver CPLEX [49].

The main contributions of this paper over the existing works in literature are summarized as follows.

- Proposing computationally-efficient MILP models for the proper automation of the HEV heterogeneous fleet considering CO_2 emissions reduction.
- Investigating the potential impact of using various HEV technologies in the service sector considering their supply of goods capacities and sustainable modes of navigation that guarantee the optimal using of the battery.
- From a sustainable standpoint, the application of this smart tool contributes to reducing dependence on fossil fuels as well as the minimization of polluting gases in urban centers.

The remainder of this work is organized as follows. The hypothesis and stochasticity in the HEVs operation are presented in Section II. Optimization models and the linearization process are presented in Section III. Section IV explains in detail the proposed methodology. Section V presents the numerical example and results. Conclusions are given in Section VI.

II. SIMULATION SETUP

In this section, first, a general explanation of the primary requirements of the automation strategy for transportation purposes is provided. Then, the main hypotheses of the proposed model, the location of charging stations and delivery points, as well as the uncertainties associated with the HEV are explained in detail.

The HEVs automation strategy should take into account the basic information [38], see Fig. 1. As can be seen, the service operators require some information of the urban areas, namely offline information such as location of the warehouse, delivery points and the number of goods to be delivered, and charging stations, and online information such as the traffic density in the urban roads [38], [39]. Then, a set of deliveries is assigned to each HEV of the fleet considering its transport capacity, i.e., the quantity of goods that the HEV can transport, and hybrid technology characteristics, e.g., SoC, battery capacity, fuel tank capacity, autonomy, etc. Fig. 2 is used to illustrate the assignment and delivery of goods, and the operational strategies in the delivery process [36]. There exist a set of deliveries, i.e., *delivery 1* to *4*, differentiable in quantities and types of goods that influence the HEV selection. The operator analyzes all the possible operational strategies and the sequences in which the goods will be delivered, the urban routes to be traversed as part of the total delivery route, i.e., *Route 1* to *5*, as well as the charging points to be visited during navigation for charging purposes [7]. Considering all these aspects during the HEV navigation, from starting and returning to the warehouse, results in a highly complex model.

A. Hypotheses

In the proposed approach, the following hypotheses are used to adequately model the problem.

1. In the urban map, the locations of all the deliveries and charging points are predefined.
2. There is only one point within the urban map that the HEVs departure and arrive, namely the warehouse.
3. Each urban road is subject to a speed limit as a consequence of uncertainties in the traffic density.
4. The costs due to the degradation of the battery present a linear behavior based on the SoC of each HEV.
5. An operation consists of a given number of delivery points to be visited.
6. An operating strategy consists of a specific sequence in which the delivery points are visited.

TABLE I
ACCUMULATED PROBABILITY RELATED TO TRAFFIC DENSITY

LOS	A			B				C			
u	1	2	3	4	5	6	7	8	9	10	11
D_u (veh/km)	5	6	7	8	9	10	11	12	13	14	15
Main urban roads ki											
P_u^{amr}	1/11	2/11	3/11	4/11	5/11	6/11	7/11	8/11	9/11	10/11	11/11
Secondary urban roads ki											
P_u^{asr}	11/11	10/11	9/11	8/11	7/11	6/11	5/11	4/11	3/11	2/11	1/11

Fig. 3. Urban map containing 412 intersections and 832 roads.

Fig. 4. Cumulative probability behavior and traffic density values for each urban road ki.

B. Location of Charging Stations and Delivery Points

In this work, to model the locations of charging stations and delivery points [36], [40] are used where the urban map presented in [36] is extended to a large-urban map, as depicted in Fig. 3. The main and secondary urban roads are differentiated by t_{ki}^{ur} and are represented by gray and dashed lines, respectively [7]. In this figure, the charging stations are presented with gray squares, and the distance between two consecutive stations is approximately five kilometers. The charging stations in the secondary roads are located at the intersections i ($r_i^s = 1$) near the main roads and by the city perimeter. The green-filled triangles and empty stand for the warehouse and delivery points, respectively. For identification of each intersection i to be visited by HEV during delivery d, parameter $t_{d,i}^n$ is used that can take two values, 1 or -1 that stand for arrival and departure intersections, respectively. Locations of the warehouse, charging, and deliveries, as well as the length of the roads on a large-urban map, are available in [41].

C. Modeling of Uncertainties

This paper considers the uncertainties correspond to the variation of traffic density (vehicle per kilometer), as a stochastic phenomenon, on a given road. The traffic density affects the speed limit of the HEVs in a road [36], [42]. Traffic density values linked to the LOS are used to simulate these uncertainties.

In practice, to represent the LOS, six letters A-F are used [43] where the difficulties that the HEV driver will have along an urban road are increased from A to F. In order to portray this

Fig. 5. Flowchart of the simulation algorithm.

stochastic difficulty, in this work, the uncertainties are simulated based on the first three usual levels such as A (low traffic density, car drivers have complete mobility on the roads), B (reasonable traffic density, slightly restricted maneuverability) and C (high traffic density, maneuverability is restricted and driver needs high concentration) [44], [45]. Table I shows the cumulative probability values to be adopted [7]. The values of P_u^{amr} or P_u^{asr} are calculated considering that each urban road ki has the same probability, e.g., as can be seen in Table 11, there exist 11 subcases in total (3 subcases in level A, 4 subcases in level B, and 4 subcases in level C), the probability is $1/11$. These probabilities are assigned to the given values of D_u. Thus, the accumulated probability values, P_u^{amr}, are obtained by adding up the probability values, P_u^{mr}, in each subcase, e.g., in subcase 3 it will be calculated as $1/11 + 1/11 + 1/11 = 3/11$, as can be seen in Table I. Therefore, in the main urban roads, the lower values of P_u^{amr} are related to a lower quantity of traveled vehicles per kilometer, D_u, while the higher probability values are considered for higher traffic density (see Fig. 4). This fact ensures the representation of higher vehicle flow on the main roads that makes the operational performance of HEVs more complex.

The cumulative probability curves of P_u^{amr} and P_u^{asr}, on the left side of Fig. 4, is used to extract the accumulated probability values of traffic density presented in Table I. This way, on the secondary urban roads, the behavior of a lower vehicle flow is related to a higher probability, thus, with a lower probability, the situations in which a secondary road presents a higher traffic density are characterized. The cumulative probability values are used to assign the density values, D_u, to all the main and secondary roads [7], [37]. Fig. 5 represents the proposed algorithm to simulate uncertainties related to traffic density variation, where v_o^{mr} and v_o^{sr} are set to 60 and 30, respectively. The number of iterations is equal to the number of roads in the urban map. This algorithm starts with pre-defined values for parameters P_u^{amr}, P_u^{asr}, D_u, D_J, v_o^{mr}, v_o^{sr}, while D_{ki} and v_{ki} are initialized to zero. Nonzero random values within interval [0,100] are assigned to n^{al}; the condition, $n^{al} \neq 0$ is evaluated to guarantee the nonzero value. Then, to start the iterative process for calculating v_{ki}, type of roads are differentiated via

checking the condition t_{ki}^{ur}. If the condition $t_{ki}^{ur}=1$ is satisfied, then the process belongs to the main roads otherwise this process is used for the secondary roads ($t_{ki}^{ur} = 0$). Note that the iterative process is similar for both roads, it is only required to consider the values correspond to them, P_u^{amr}/P_u^{asr} and v_o^{sr}/v_o^{mr}. Therefore, the detail explanation of this iterative process is provided for the main roads. If $u=1$, n^{al} is assessed under the condition $0 \leq n^{al} \leq P_u^{amr}$, and if this condition is satisfied, D_u is assigned to D_{ki} and v_{ki} is obtained. Otherwise, for $u>1$, the condition $P_{u-1}^{amr} \leq n^{al} \leq P_u^{amr}$ is used to evaluate n^{al}, and if this condition is satisfied, D_{ki} is assigned to its respective D_u and v_{ki} is calculated. This internal iterative process terminates when the stopping criterion $u=|\Omega_D|$ is met, and then the algorithm checks whether the process has been done for all roads. At the end of this iterative process, the values of v_{ki} for each road ki on the urban map are obtained. This value is used in the first term of (1).

III. PROPOSED MODEL

In this section, the mathematical formulation of the proposed two-stage model is presented in detail.

A. First-stage: MINLP Model

The problem of this stage is represented via a mixed-integer nonlinear programming (MINLP) model (1)–(16).

$$min: \ \delta^{nt}\varphi_1 + \delta^{bl}\varphi_2 \tag{1}$$

where,

$$\varphi_1 = \sum_{\forall d \in \Omega_d} \sum_{\forall ki \in \Omega_{ur}} \omega_{e,d,ki}\left(\frac{l_{ki}}{v_{ki}}\right)$$

$$\varphi_2 = \sum_{\forall d \in \Omega_d} \sum_{\forall i \in \Omega_i} C^B\left(\frac{mSOC_{e,d,i} - b}{8760 C^F B^L}\right)$$

subject to:

$$\sum_{\forall ki \in \Omega_{ur}} \omega_{e,d,ki} - \sum_{\forall ij \in \Omega_{ur}} \omega_{e,d,ij} = \beta,$$
$$\forall d \in \Omega_d, \forall i \in \Omega_i / t_{d,i}^n = \beta \tag{2}$$

$$l_{ki}\omega_{e,d,ki} = l_{e,d,ki}^{CDM} + l_{e,d,ki}^{CSM}, \forall d \in \Omega_d, \forall ki \in \Omega_{ur} \tag{3}$$

$$0 \leq l_{e,d,ki}^{CDM}, \forall d \in \Omega_d, \forall ki \in \Omega_{ur} \tag{4}$$

$$0 \leq l_{e,d,ki}^{CSM}, \forall d \in \Omega_d, \forall ki \in \Omega_{ur} \tag{5}$$

$$\left(\frac{1}{\delta_e^C}\right) \sum_{\forall d \in \Omega_d} \sum_{\forall ki \in \Omega_{ur}} l_{e,d,ki}^{CSM} \leq \rho^C K^C \tag{6}$$

$$SOC_{e,d,i} = SOC_e^o,$$
$$\forall d \in \Omega_d, \forall i \in \Omega_i / d = 1 \wedge t_{d,i}^n = -1 \tag{7}$$

$$SOC_{e,d,i} = SOC_{e,d-1,i},$$
$$\forall d \in \Omega_d, \forall i \in \Omega_i / d > 1 \wedge t_{d,i}^n = -1 \wedge t_{d-1,i}^n = 1 \tag{8}$$

$$SOC_{e,d,i} = SOC_{e,d,i}^a + \varepsilon_{e,d,i}, \forall d \in \Omega_d, \forall i \in \Omega_i / t_{d,i}^n \geq 0 \tag{9}$$

$$SOC_{e,d,i} = \delta_e^{PE} B_e, \forall d \in \Omega_d, \forall i \in \Omega_i / d = N^d \wedge t_{d,i}^n = 1 \tag{10}$$

$$0 \leq SOC_{e,d,i} \leq B_e, \forall d \in \Omega_d, \forall i \in \Omega_i \tag{11}$$

$$SOC_{e,d,i}^a = \sum_{\forall ki \in \Omega_{ur}} \omega_{e,d,ki}\left(SOC_{e,d,k} - \eta^{dE}\delta_e^D l_{e,d,ki}^{CDM}\right),$$
$$\forall d \in \Omega_d, \forall i \in \Omega_i \tag{12}$$

$$0 \leq SOC_{e,d,i}^a, \forall d \in \Omega_d, \forall i \in \Omega_i \tag{13}$$

$$\varepsilon_{e,d,i} = 0,$$
$$\forall d \in \Omega_d, \forall i \in \Omega_i$$
$$/(d = 1 \wedge t_{d,i}^n = -1) \vee (t_{d,i}^n \geq 0 \wedge r_i^s = 0) \tag{14}$$

$$\varepsilon_{e,d,i} = \eta^{cE} P_e^{ch} y_{e,d,i} \tau_{e,d,i}^{ch}, \tag{15}$$

$$\forall d \in \Omega_d, \forall i \in \Omega_i / t_{d,i}^n \geq 0 \wedge r_i^s = 1$$
$$\underline{\tau}^{ch} \leq \tau_{e,d,i}^{ch} \leq \overline{\tau}^{ch}, \forall d \in \Omega_d, \forall i \in \Omega_i \tag{16}$$

The objective function (1) represents two parts related to φ_1 and φ_2, as well as their respective weighting factors. φ_1 stands for the total navigation time of each HEV and its minimization ensures that the shortest route is selected considering the traffic information represented by the speed value, v_{ki}, in each road ki to be selected as part of an operation strategy. On the other hand, φ_2 is related to the lifetime of the HEV battery, taking into account the minimization of the degradation effect due to frequent recharging. Thus, for the efficient usage of an HEV battery, an optimal level of SoC should be considered. The scheduling of deliveries d for each HEV, are made via (2). In this constraint, the values of β (−1, 0, and 1) define the type of intersection i and are used to determine the shortest route ij (related to node i) to be traveled. For $\beta = -1$, (2) is used to calculate the shortest distance l_{ij} to be traveled, from intersection i ($t_{d,i}^n = -1$) to all possible intersections j. For $\beta = 0$, (2) stands for the navigation of HEV on the roads with intermediate intersections, where the trip from intersections k to i and i to j is part of the minimum route, l_{ki} and l_{ij}. In this case, the intermediate intersections i ($t_{d,i}^n = 0$) stand for the arrival intersection of an HEV that is coming from intersections k, while at the same time, it plays the role of the departure point for the HEV going to intersections j. For $\beta = 1$ the road ki is traveled, starting from all possible intermediate intersections k ($t_{d,k}^n = 0$) to the arrival intersection i ($t_{d,i}^n = 1$), where, l_{ki} represents the shortest road. Constraints (3)-(6) stand for the navigation modes of the HEV considering a percentage of daily fuel consumption, ρ^C. Constraint (3) shows that the distance for delivery d in each road, l_{ki}, is equal to the sum of the distances traveled in CDM, $l_{e,d,ki}^{CDM}$ and, in CSM, $l_{e,d,ki}^{CSM}$. The reduction of $l_{e,d,ki}^{CDM}$ implies a reduction in the maintenance costs of the battery (improving its lifetime), which results in increasing $l_{e,d,ki}^{CSM}$, and consequently, more fuel is consumed and higher CO_2 is emitted. However, to ensure the sustainable management of the fleet, it is necessary to consider a daily fuel consumption limit that allows the efficient use of the battery taking into account the minimization of the effects of degradation during its lifetime. Constraints (4) and (5) stand for non-negativity conditions. The distance traveled in CSM, $l_{e,d,ki}^{CSM}$, considering ρ^C is guaranteed in (6). Note that CO_2 emissions are implicitly limited when a daily fuel consumption, $\rho^C K^C$, is considered. Therefore, the energy of HEV battery is used more frequently (obtaining a longer distance traveled in CDM, $l_{e,d,ki}^{CDM}$), in order to optimize its useful lifetime. The battery charging of each type of HEV is established via (7)-(16). In (7), the initial SoC at intersection i ($t_{d,i}^n = -1$) is considered for the first delivery d. At intersection i, the SoC of HEV e in delivery d, ($t_{d,i}^n = -1$), is equal to its SoC in delivery $d-1$, ($t_{d-1,i}^n = 1$), (8). The SoC for delivery d at intersection i ($t_{d,i}^n \geq 0$) is calculated by (9). To do so, the available energy, $SOC_{e,d,i}^a$, and the recharging energy by the HEV at the charging station i ($r_i^s = 1$), $\varepsilon_{e,d,i}$, is considered. For the final SoC at intersection i, ($t_{d,i}^n = 1$), after returning to the

TABLE II
OPERATING STRATEGIES RELATED TO OPERATION 1

e	s	v	Warehouse and delivery points d
1	**1**	**1**	: $214 \rightarrow 211 \rightarrow 250 \rightarrow 265 \rightarrow 276 \rightarrow 214$
2	**2**	**2**	: $214 \rightarrow 211 \rightarrow 250 \rightarrow 276 \rightarrow 265 \rightarrow 214$
3	**3**	**3**	: $214 \rightarrow 211 \rightarrow 265 \rightarrow 250 \rightarrow 276 \rightarrow 214$
4	**4**	**4**	: $214 \rightarrow 211 \rightarrow 265 \rightarrow 276 \rightarrow 250 \rightarrow 214$
	⋮		⋮
	11	**11**	: $214 \rightarrow 250 \rightarrow 276 \rightarrow 211 \rightarrow 265 \rightarrow 214$
	12	**12**	: $214 \rightarrow 250 \rightarrow 276 \rightarrow 265 \rightarrow 211 \rightarrow 214$
	⋮		⋮
		24	: $214 \rightarrow 276 \rightarrow 265 \rightarrow 250 \rightarrow 211 \rightarrow 214$

TABLE III
MAIN FEATURES OF THE HEV TECHNOLOGY TYPES

HEV e	C_e^{HEV} (units)	SOC_e^o (kWh)	δ_e^C (km/L)	B_e (kWh)	au_e (km)	$E_e^{CO_2}$ (gCO$_2$/Km)	δ_e^D (kWh/Km)
1	15	8.8	71.43	8.8	35	32	0.201
2	20	18	29.42	18	80	40	0.180
3	10	6.7	41.67	6.7	21	148	0.255
4	13	16	40.00	16	80	27	0.160

warehouse ($d = N^d$) (10) is used, while (11) guarantees the limits of $SOC_{e,d,i}$. In (12), $SOC_{e,d,i}^a$ is obtained as the difference between $SOC_{e,d,k}$ at intersection k and the energy used during the trip in CDM on road ki ($\omega_{e,d,ki}=1$), $\eta^{dE}\delta_e^D l_{e,d,ki}^{CDM}$. Constraint (13) stands for the non-negativity condition of $SOC_{e,d,i}^a$. To avoid charging at the starting intersection i ($t_{d,i}^n = -1$), during the first delivery, and for the subsequent deliveries with intersection i ($t_{d,i}^n \geq 0$) in which there is no charging station ($r_i^s = 0$), (14) is used. The recharge energy, $\varepsilon_{e,d,i}$, is calculated in (15) which depends on the variables $y_{e,d,i}$ and $\tau_{e,d,i}^{ch}$ at intersection i which is equipped with charging station, $r_i^s = 1$. Constraint (16) guarantees that $\tau_{e,d,i}^{ch}$ within the acceptable bounds.

B. Second-stage: MILP Model

The proposed approach at this stage is presented by an MILP model, (17)–(20).

$$min: \delta^{ue}\Delta C^{HEV} + \sum_{\forall e \in \Omega_e} \sum_{\forall s \in \Omega_{op}} \sum_{\forall v \in \Omega_{ps}} M_{e,s,v}^{fob} Z_{e,s,v} \quad (17)$$

subject to:

$$\sum_{\forall s \in \Omega_{op}} \sum_{\forall v \in \Omega_{ps}} Z_{e,s,v} \leq |\Omega_{op}|; \ \forall e \in \Omega_e \quad (18)$$

$$\sum_{\forall e \in \Omega_e} \sum_{\forall v \in \Omega_{ps}} Z_{e,s,v} = 1; \forall s \in \Omega_{op} \ / U_s^{op} \leq C_e^{HEV} \quad (19)$$

$$\sum_{\forall v \in \Omega_{ps}} \left(\sum_{\forall e \in \Omega_e} \sum_{\forall s \in \Omega_{op}} C_e^{HEV} Z_{e,s,v} - \sum_{\forall s \in \Omega_{op}} \sum_{\forall e \in \Omega_e} U_s^{op} Z_{e,s,v} \right) \leq \Delta C^{HEV} \quad (20)$$

The objective function at this stage (17) is composed of two terms. The first term stands for the costs related to the total quantity of extra goods obtained as a result of the optimal management of the operations of the heterogeneous fleet. The second term represents the values of the objective functions obtained for HEV e in operation s via the possible strategy v. In this term, the cost matrix $M_{e,s,v}^{fob}$ is obtained from the first stage.

Constraint (18) guarantees the limit of the number of operations to be performed by a type of HEV technology, while (19) guarantees that only one strategy is possible to be selected in operation s of a type of HEV e, so that the capacity, C_e^{HEV}, is greater than or equal to the total demand, U_s^{op}. The balance

Fig. 6. Flowchart of the iterative process.

between the total capacity of transporting goods by the HEV heterogeneous fleet and the total demands in operation s, U_s^{op}, is established in (20). This balance is related to the number of extra units of goods, ΔC^{HEV}, to be minimized in (17).

C. Linearization

The global solution of the proposed MINLP model in the first stage cannot be guaranteed via existing commercial solvers, although a well-defined nonlinear model may result in a high-quality optimal solution [46]. Therefore, an appropriate linearization technique, the Big-M method, is applied to recast the nonlinear terms in (12) and (15), [47].

Constraint (12) is replaced with (21.a) and the linearization technique presented in [7] is used in (21.b)-(21. e).

$$SOC_{e,d,i}^a = \sum_{\forall ki \in \Omega_{ur}} \left(\Delta_{e,d,ki}^{'} - \delta_e^D \Delta \omega_{e,d,ki}^{CDM} \right), \quad (21.a)$$
$$\forall d \in \Omega_d, \forall ki \in \Omega_{ur}$$

$$0 \leq -\Delta_{e,d,ki}^{'} + SOC_{e,d,k} \leq M * \left(1 - \omega_{e,d,ki} \right), \quad (21.b)$$
$$\forall d \in \Omega_d, \forall ki \in \Omega_{ur}$$

$$0 \leq \Delta_{e,d,ki}^{'} \leq M\omega_{e,d,ki}, \forall d \in \Omega_d, \forall ki \in \Omega_{ur} \quad (21.c)$$

$$0 \leq -\Delta\omega_{e,d,ki}^{CDM} + l_{e,d,ki}^{CDM} \leq M\left(1 - \omega_{e,d,ki}\right), \quad (21.d)$$
$$\forall d \in \Omega_d, \forall ki \in \Omega_{ur}$$

$$0 \leq \Delta\omega_{e,d,ki}^{CDM} \leq M\omega_{e,d,ki}, \forall d \in \Omega_d, \forall ki \in \Omega_{ur} \quad (21.e)$$

To linearize (15), constraints (22.a)-(22.c) are used.

$$\varepsilon_{e,d,i} = \eta^{cE} P_e^{ch} \Delta\tau_{e,d,i}^{ch}, \quad (22.a)$$
$$\forall d \in \Omega_d, \forall i \in \Omega_i / t_{d,i}^n \geq 0 \wedge r_i^s = 1$$

$$0 \leq -\Delta\tau_{e,d,i}^{ch} + \tau_{e,d,i}^{ch} \leq M\left(1 - y_{e,d,i}\right), \forall d \in \Omega_d, \forall i \in \Omega_i \quad (22.b)$$

$$0 \leq \Delta\tau_{e,d,i}^{ch} \leq My_{e,d,i}, \forall d \in \Omega_d, \forall i \in \Omega_i \quad (22.c)$$

D. MILP models

The obtained MILP models are as follows.
First Stage: *min* (1) s.t.: (2)-(11), (13)-(14), (16), (21), (22).
Second Stage: *min* (17) s.t.: (18), (19), (20).

IV. PROPOSED METHODOLOGY

This section provides detailed explanations of the proposed methodology.

A. First Stage

At this stage, the optimization problem related to the objective function (1) is solved as a part of the iterative process depicted in Fig. 6 using the hyper-matrix data, $M_{e,s,v,d}^{del}$, to
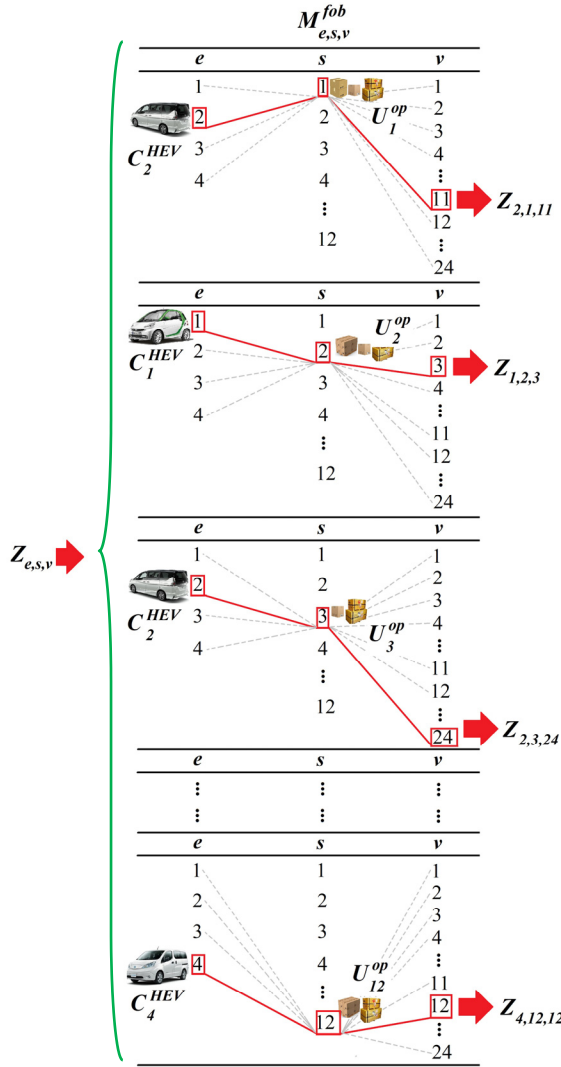
Fig. 7. Selection of HEV e and operating strategy v for each operation s.

obtain the $M_{e,s,v}^{fob}$ values. Table II shows the structure of this hyper-matrix related to operation 1 with delivery points in the intersections 211, 250, 265, and 276 [41]. For this operation, all possible strategies v for a given HEV e are presented. Also, all the operating strategies v start and end at intersection 214, which is the warehouse. In matrix $M_{e,s,v}^{fob}$, obtained via the iterative process, each element represents the value of the objective function (1) for each strategy v of the operation s to be performed by HEV e. The iterative process is run for each type of HEV technology to be used for operation s considering all the operating strategies v. The algorithm starts with pre-established values: Ω_e, Ω_{op}, Ω_{ps}, Ω_d, Ω_i, and $M_{e,s,v,d}^{del}$. The values $t_{d,i}^n$ and $M_{e,s,v}^{fob}$, are initialized to zero. Table III anonymously presents the information related to the types of HEVs. Real data of 4 different existing technologies are anonymously used.

In addition, another iterative process is executed to each delivery d and, intersection i. All intersections i are compared under conditions $i = M_{e,s,v,d}^{del}$, and $i = M_{e,s,v,d+1}^{del}$. Depending on the value of intersection i (which exist in the matrix $M_{e,s,v,d}^{del}$), the conditions can be met or not, and consequently, -1 (stands

for departure) and 1 (stands for arrival) are assigned to $t_{d,i}^n$, respectively. Thereafter, the condition $i = |\Omega_i|$, is evaluated for each intersection i. If this condition is not met, then a new iteration for i is performed, otherwise, condition $d = |\Omega_d|$ is considered for each d; if this condition is not met, then the iteration is performed for the next d. Otherwise, the proposed MILP model is solved and the solution is assigned to $M_{e,s,v}^{fob}$. Then, for each operating strategy v, condition $v = |\Omega_{ps}|$ is evaluated. If the condition is not met, then a new iteration for v is done, otherwise, the condition $s = |\Omega_{op}|$ is evaluated for each s. If this condition is not met, then the iteration is done for the next operation s. Otherwise, the MILP model is solved for another HEV e technology considering the condition $e = |\Omega_e|$, and if this condition is not met, the iteration for the next e is done, otherwise, the process terminates. Up to this point, the best fleet automation strategy without considering goods capacity of HEVs is determined by the summation of the minimum values of the matrix of the objective function related to operating strategy v for operation s of HEV e, $M_{e,s,v}^{fob}$. Note that this minimum value is strongly tied to each operating strategy v to be made by HEV e, which presents the minimal navigation time as well as the most economical battery usage. To ensure that the heterogeneous fleet automation strategy is not only sustainable but also operationally efficient in terms of the number of goods to be transported (see Figs. 1 and 2), a second stage that optimizes the vehicles transport capabilities is implemented based on information from the matrix $M_{e,s,v}^{fob}$.

B. Second Stage

In the MILP model with objective function (17), ΔC^{HEV} and $Z_{e,s,v}$ are decision-making variables at this stage. In this objective function, the $M_{e,s,v}^{fob}$ values calculated in the previous stage serve as the coefficients related to the main variable $Z_{e,s,v}$. Fig. 7 provides an illustrative example of selecting the best operational strategy among all for each operation s via variable $Z_{e,s,v}$. If operation s equals 1 ($Z_{2,1,11} = 1$), operating strategy 11 and HEV with technology type 2 are selected, while, for operations 2 ($Z_{1,2,3} = 1$) and 3 ($Z_{2,3,24} = 1$), the HEV types 1 and 2 under operating strategies 3 and 24 are selected, respectively. An interesting observation is that for two different operations, e.g., 1 and 3, the same type of vehicular technology can be used as far as the capacity of this vehicle meets the requirements of each operation s. Note also that, at this stage, the $C_e^{HEV} Z_{e,s,v}$ and $U_s^{op} Z_{e,s,v}$ terms play a key role in efficiently managing the HEVs capability in goods delivery, that is, reducing the values of ΔC^{HEV} for the heterogeneous fleet so that the maximum capacity to be used while not overloading the HEVs. This way variable $Z_{e,s,v}$ allows us to select the best type and strategy to carry out a given operation guaranteeing the optimal management of the heterogeneous fleet of HEVs.

V. RESULTS AND DISCUSSION

In order to evaluate the proposed two-stage model, the urban area presented in Fig. 3 is used for tests. Twelve operations ($|\Omega_{op}| = 12$) are considered in which four different delivery points should be visited for each operation [41]. Each operation s presents 24 operating strategies ($|\Omega_{ps}| = 24$) representing the possible sequences in which an HEV can perform the
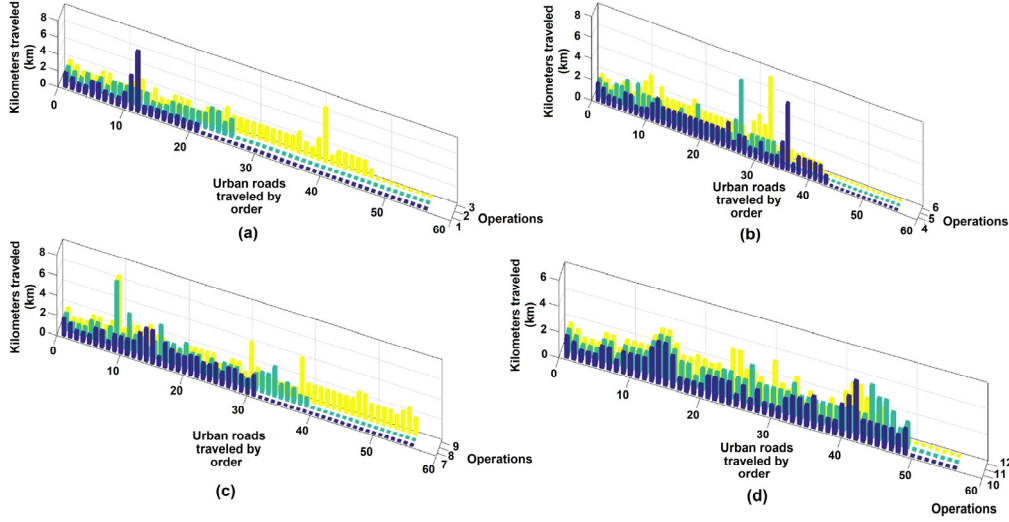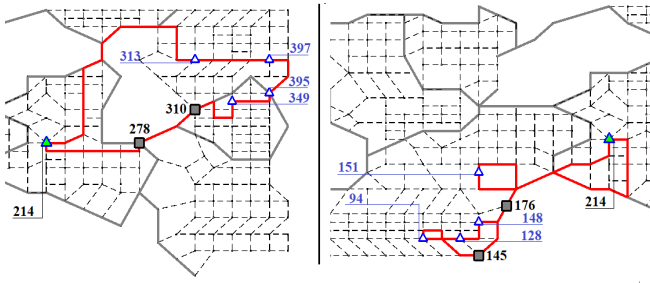
Fig. 8. Urban roads traveled in each operation.

TABLE IV
OPTIMAL MANAGEMENT SCHEME OF THE HEV HETEROGENEOUS FLEET

$s\ (U_s^{op})$	$e(C_e^{HEV})$	Nº	Best operating strategies	With CDM/CSM (L)	Without CDM/CSM (L)
1 (15)	1 (15)	12	214→250→276→265→211→214	0.11	0.43
2 (14)	1 (15)	16	214→254→227→259→207→214	0.22	0.54
3 (13)	4 (13)	1	214→248→282→315→400→214	0.46	1.79
4 (12)	1 (15)	6	214→313→397→395→349→214	0.29	0.90
5 (10)	3 (10)	4	214→321→363→366→325→214	0.79	1.22
6 (16)	2 (20)	10	214→304→360→381→292→214	0.59	2.31
7 (17)	2 (20)	1	214→156→166→189→199→214	0.88	1.76
8 (13)	1 (15)	19	214→151→94→128→148→214	0.40	0.90
9 (12)	1 (15)	15	214→34→21→5→63→214	0.65	1.26
10 (13)	1 (15)	24	214→140→86→71→51→214	0.47	1.08
11 (11)	4 (13)	1	214→27→29→53→55→214	0.78	2.21
12 (20)	2 (20)	1	214→ 57→125→162→184→214	0.99	2.72

deliveries. Also, 4 types of HEV technologies ($|\Omega_e| = 4$) are considered, as shown in Table III. The $M_{e,s,v,d}^{del}$ values related with the operating strategies are shown in Table II. At the first stage, the iterative process presented in Fig. 6 is run. The values of v_{ki} are obtained via the algorithm portrayed in Fig. 5. The value of δ_e^D for each HEV type is $0.8K^E$ divided by au_e. The SOC_e^o of HEV e is equal to the battery capacity, B_e, while δ_e^{PE} for the arrival is set to 85%. All the HEVs start with $K^C = 40$L, and the fuel price is considered to be \$3.65/L [7]. For each charging point, the values P_e^{ch}, $\underline{\tau}^{ch}$, and $\overline{\tau}^{ch}$, are set to 10 kW, 0.3 h, and 0.5 h, respectively [20], [36]. The efficiencies, η^{cE} and η^{dE} are considered to be 0.98 and 1.00, respectively [8], [29]. The daily fuel consumption, ρ^C, is set to 30% [29]. The weighting coefficients δ^{nt}, δ^{bd}, δ^{ue}, are set to 100, 10, and 1, respectively. It is worth highlighting that the coefficients related to the optimization model in the first stage present a greater weight, specifically, the coefficient related to the total navigation time of the fleet. Reducing the navigation time of the HEV fleet results in efficiently managing both the charging time and the number of times that the battery needs to be recharged. Thus, in our proposed methodology, the best operational strategies with the minimum navigating time are guaranteed. In order to consider a linear degradation of the batteries of the HEV fleet, m and b adopt the respective values

of 1.59e^{-6} and 6.41e^{-6}. In addition, B^L is 10 years, the capacity fade at the end of life, C^F, and the battery cost, C^B, for each HEV are 0.2 and \$300/kWh, respectively [21]. In the second stage, the values of U_s^{op}, and C_e^{HEV} are shown in Table IV. The programming language AMPL is used for the implementation purpose, while the global optimal is obtained via the commercial solver CPLEX on a PC with 2.67-GHz CPU, and 3 GB of RAM. Table IV shows the type of HEV technology, the best operating strategy selected for each operation and the fuel consumption for two cases: with and without CDM/CSM. The term *without CDM/CSM* refers to the condition in which HEV e only navigates in CSM (charge-sustaining mode), i.e., the HEV is propelled by the energy produced by the fuel consumption, while the term *with CDM/CSM* stands for the conditions in which the HEV can select between CSM and CDM (charge depleting mode), i.e., the HEV is propelled by the energy produced by either the fuel consumption or the energy stored in the battery. Each operation is supplied by a type of HEV with $C_e^{HEV} \geq U_s^{op}$, ensuring that each HEV satisfies the capacity limit in transporting the goods. Thus, the total extra goods units, ΔC^{HEV}, in each HEV related to operations 2, 4, 6, 7, 8, 9, 10 and 11, resulting in 20 units. For example, in scenario 1, the capacity of HEV type *1* is 15 and it is carrying 15 goods, while in scenario 6, the capacity of HEV type *2* is 20 and it is carrying only 16 goods, resulting in 4 extra vacant lots. The total costs regarding fuel consumption for both cases are \$24.20 and \$62.49, which show savings of 61.27% per day. It is worth mentioning that, for each operation, the values of *with CDM/CSM* and *without CDM/CSM* have been calculated considering the same shortest route related to the best operational strategy. In order to know the characteristics of the driving routes of the operations carried out by the heterogeneous fleet, the sequence of urban roads ki traversed by each HEV during operation is shown in Fig. 8. In this figure, each subfigure contains the operation number (in the right-side of vertical direction), number of traversed urban roads during the operation (in horizontal direction), and the traveled distances (in the left-side of vertical direction). As can be seen, all the vehicles have traversed below 60 urban roads while,

Operation 4: 214 -> 313 -> 397 -> 395 -> 349 -> 214   Operation 8: 214 -> 151 -> 94 -> 128 -> 148 -> 214

Fig. 9. Routes related to the operations 4 and 8.

TABLE V
CHARACTERISTICS OF URBAN ROADS TRAVERSED IN EACH OPERATIONAL STRATEGY

Operation s	Total distance (km)	Total Distance (%)	Longest Urban road ki	Total # of Urban roads
1	30.88	34.28	7.2	21
2	38.40	42.63	2.56	26
3	71.52	79.40	6.4	47
4	64.64	71.76	6.4	43
5	50.72	56.31	6.4	34
6	67.84	75.31	7.2	41
7	51.84	57.55	3.2	31
8	64.64	71.76	6.4	39
9	90.08	100.0	6.4	56
10	77.44	85.97	4.48	49
11	88.48	98.22	4.00	49
12	80.16	88.99	3.20	45

Operation 3: 214->248->282->315->400->214
Operation 9: 214-> 34-> 21-> 5-> 63->214
Operation 5: 214->321->363->366->325->214
Operation 12: 214-> 57->125->162->184->214
(a)   (b)

Fig. 10. Routes related to the representative efficient strategies.

Fig. 11. Kilometers traveled by HEVs related to the representative cases.

among all, the largest and smallest number of traversed urban roads belong to operation 9, with 56 traversed roads, and operation 1, with 21 traversed roads, respectively. In this figure, the longest urban road (7.2 km) is traversed by the HEV of type 1 during operation 1, see Fig. 8 (a). From Fig. 8 (d), it can be seen that in operations 10 and 11, the total number of traversed urban roads is similar, 49 for each. To see the difference between these two cases, Table V is presented. Features such as the total distance, longest urban road, and the total number of urban roads traversed within the best operational strategies, presented in Table IV, are detailed in Table V. In this table, the percentages are obtained with respect to the largest traveled distance that belongs to operation 9. From this table, it can be concluded that the traveled distance in operation 10, is 77.44 km, which is a bit lower than the distance traveled in operation 10, with 88.48 km. Moreover, it can be seen that the total distances related to operations 4 and 8 are similar, 64.64 km. However, the number of urban roads traversed in operation 4 is more than the one in operation 8, see Table V. Fig. 9 is used to illustrate the number of urban roads traversed by the HEV to do the deliveries while visiting the charging points, if necessary.

In addition, the shape of these types of routes can be used to explain the strong influence of traffic density as well as the driving direction (one-way or two-way) during navigation. For example, in operation 8, HEV departs from the warehouse (node 214) to arrive at the first delivery location (node 151); among these nodes there are several paths that could have been selected as part of the total route, but due to the influence of the aforementioned factors, the most practical choice is the red path. In order to analyze the most representative cases of Table IV, Fig. 10 shows the shortest routes related to the best operating strategies selected for operations 3, 5, 9, and 12, performed by different types of HEVs. The charging points to be visited by an HEV are represented by gray squares. In Fig.
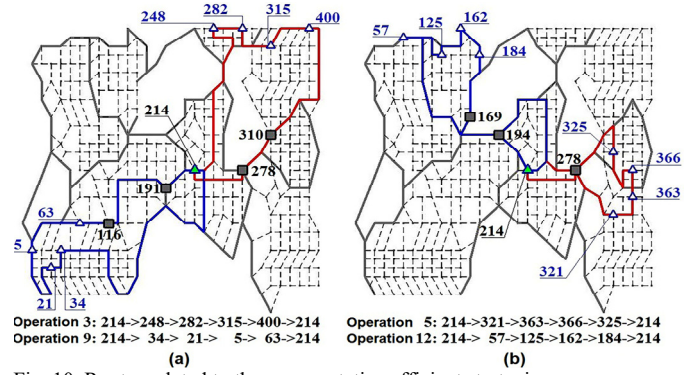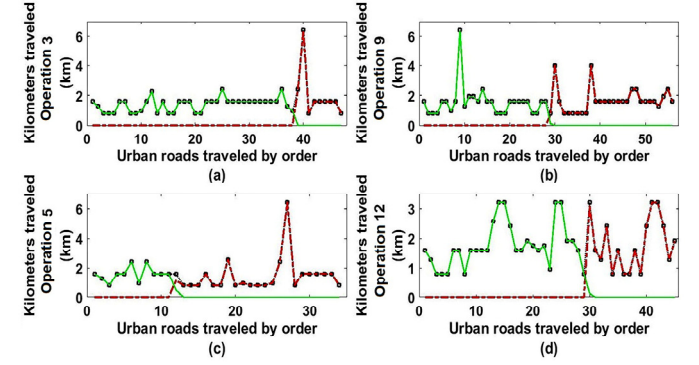
10 (a), the shortest routes related to the operations 3 (red line) and 9 (blue line) are shown. Note that for both routes, the HEVs of type 4 and 9 recharge their batteries at the charging points 278 and 310, and 116 and 191, with charging times of 0.5 h and 0.43 h, and 0.47 h and 0.50 h, respectively. This fact shows that, for operations with deliveries located far away from the warehouse location, the best decision of the fleet operator should consider the use of HEVs with higher battery capacities and autonomy. Fig. 10 (b) shows the routes to be traveled by the HEVs of type 3 and 2 related to operations 5 (red line) and 12 (blue line), respectively. Note that the HEV of type 2 visits more charging points (169 and 194, both with charging times of 0.5 h), compared to the HEV of type 3 (278 with 0.5 h). It is worth mentioning that the recharge done by the HEV of type 3 occurs during the return to the warehouse. Also, operation 9 (90.1 km), with the highest number of km, is performed by the HEV of type 1 (8.8 kWh) with battery recharges at charging points (116 and 191) with a longer distance than the other cases, i.e., the distance between 116 and 191 is longer than the distance between 278 and 310 or 169 and 194. In this case, for the HEV with lower energy storage capacity, the strategy chooses to charge the battery at a lower number of charging points with a longer distance and not to charge at more charging points with shorter distances. These representative cases reveal the impact of optimal management of HEVs for a given daily operation and emphasize the importance of implementing heterogeneous fleets with different operational characteristics within the service sector. Figs. 11 (a)-(d) show the CDM/CSM of the HEVs related to the representative cases by setting ρ^c to 30%. The black dots represent the distances of each road ki traveled by HEVs during the navigation on the shortest route without considering the CDM/CSM, $l_{ki}\omega_{e,d,ki}$, while the
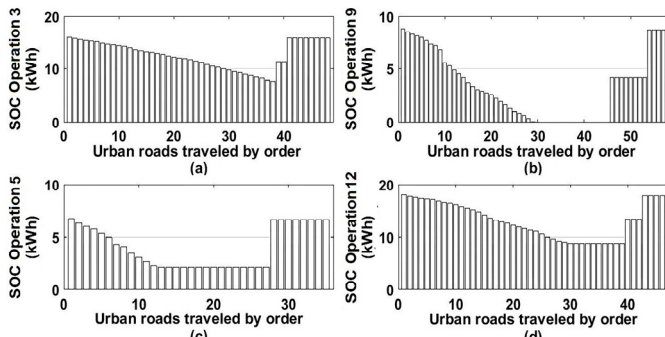
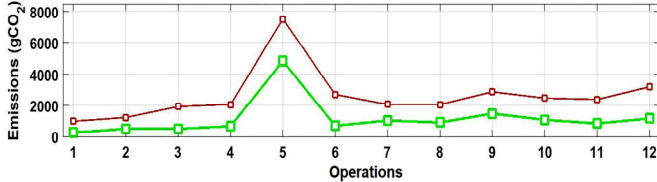Fig. 12. The SoC profile of the HEVs related to the representative cases.

Fig. 13. Reduction of CO_2 emissions of the HEV fleet.

distances traveled in CSM ($l_{e,d,ki}^{CSM}$) and CDM ($l_{e,d,ki}^{CDM}$) are presented by the red-dashed and green lines, respectively, for the case with CDM/CSM. The values in which the black dots and green lines meet each other indicate that the HEV has navigated in CDM, i.e., with an efficient use of the battery energy. Otherwise, the HEV has navigated some distance in CSM and the remaining distance in CDM. Note that from the beginning of each operation, most of the roads are traveled in CDM and the remaining distances are traveled in CSM; then fully charged batteries are available for the next operation, as shown in Fig. 12. Figs. 12 (a)-(d) show the SoC profiles of the HEVs for different operations considering the efficient battery charging.

The decreasing bars represent SoC values when the vehicle has used the battery power in CDM from the beginning of the operation. The bars with constant values indicate the fuel consumption by the HEV in CSM, after an efficient use of the battery. The bar changes from one constant level to another, which indicates that the HEV battery is charging at these points. In Figs. 12 (a), (b) and (d), there are two jumps for each operation. For operation 3, the jumps are from 7.65 kWh to 11.34 kWh and from 11.34 kWh to 15.84 kWh; for operation 9, from 0 kWh to 4.21 kWh and from 4.21 kWh to 8.71 kWh; and for operation 12, from 8.82 kWh to 13.32 kWh and from 13.32 kWh to 17.82 kWh. Fig. 12 (c) shows a jump for operation 5, from a level of 2.13 kWh to 6.63 kWh. These facts demonstrate the applicability of HEV technology in the service sector ensuring the sustainable operation of the heterogeneous fleet. Fig. 13 shows the reduction of CO_2 emission levels obtained as a selection of the best strategies related to each operation presented in Table IV. The CO_2 emission level values for the operation of HEVs with and without CDM/CSM are shown with green and red lines, respectively. The total contribution of the reduction of CO_2 emissions by the HEV fleet reaches a value of 55.7% with respect to the total emissions obtained without CDM/CSM, which is a considerable reduction. Note that operation 5, where a shorter distance is traveled in CDM, presents a higher emission reduction due to the high value of

$E_e^{CO_2}$ related to the HEV of type 3 (see Table III). The positive impact of the optimal management of the HEVs in urban areas is evidenced as a consequence of the significant reduction of polluting emissions.

VI. CONCLUSIONS

In this paper, a two-stage methodology has been proposed for the efficient automation of an HEV heterogeneous fleet. In the first stage, the deliveries scheduling, CDM/CSM driving mode strategies, and SoC of the HEV battery for a given percentage of CO_2 emission reduction has been considered. However, finding the optimal operating strategy among all the possible operating strategies, the HEV to be assigned for each operation, while considering its capacity, has been handled in the second stage. The MILP models associated with the two stages of the proposed framework are subject to a set of operational and environmental constraints while considering deliveries schedules, speed variation, battery, and fuel capacities, distances traveled in CDM and CSM, charging and discharging rates, emission reduction levels, and the goods units to be delivered by various HEV technologies. The speed variation is presented by the probability values associated with the LOS. An urban area that contains 412 intersections and 832 roads has been used for the optimal management of the HEV heterogeneous fleet aimed at obtaining the minimum operational cost. Results show that the proposed methodology is advantageous in analyzing and enhancing the operational performances in navigation systems of HEV fleet with different technologies by allowing companies in the service sector to address economic and sustainable criteria by encouraging the use of clean alternative sources instead of relying on fossil fuels.

REFERENCES

[1] "US Energy Information Administration (EIA), Annual Energy Outlook 2019 with projections to 2050," 2019. [Online]. Available: https://www.eia.gov/outlooks/aeo/pdf/aeo2019.pdf.

[2] "UPS Sustainability, On the Leading Edge: The UPS Corporate Sustainability Progress Report," 2017. [Online]. Available: https://sustainability.ups.com/media/2017_UPS_CSR.pdf.

[3] S. Rajakaruna, F. Shahnia, and A. Ghosh, *Plug In Electric Vehicles in Smart Grids*. Singapore: Springer Singapore, 2015.

[4] S. Mehar, S. Zeadally, G. Remy, and S. M. Senouci, "Sustainable Transportation Management System for a Fleet of Electric Vehicles," *IEEE Trans. Intell. Transp. Syst.*, vol. 16, no. 3, pp. 1401–1414, Jun. 2015.

[5] N. C. Onat, M. Kucukvar, and O. Tatari, "Conventional, Hybrid, Plug-in Hybrid or Electric Vehicles? State-based Comparative Carbon and Energy Footprint Analysis in the United States," *Appl. Energy*, vol. 150, pp. 36–49, Jul. 2015.

[6] J. Munkhammar and M. Shepero, "Autonomous electric vehicle fleet charging in cities: Optimal utility estimates and Monte Carlo simulations," in *2017 IEEE PES Innovative Smart Grid Technologies Conference Europe (ISGT-Europe)*, 2017, pp. 1–6.

[7] F. V. Cerna, M. Pourakbari-Kasmaei, J. Contreras, and L. A. Gallego, "Optimal Selection of Navigation Modes of HEVs Considering CO 2 Emissions Reduction," *IEEE Trans. Veh. Technol.*, vol. 68, no. 3, pp. 2196–2206, Mar. 2019.

[8] C.-K. Chau, K. Elbassioni, and C.-M. Tseng, "Drive Mode Optimization and Path Planning for Plug-In Hybrid Electric Vehicles," *IEEE Trans. Intell. Transp. Syst.*, vol. 18, no. 12, pp. 3421–3432, Dec. 2017.

[9] X. Bi and W. K. S. Tang, "Logistical Planning for Electric Vehicles Under Time-Dependent Stochastic Traffic," *IEEE Trans. Intell. Transp. Syst.*, pp. 1–11, 2018.

[10] E. Yudovina and G. Michailidis, "Socially Optimal Charging Strategies for Electric Vehicles," *IEEE Trans. Automat. Contr.*, vol. 60, no. 3, pp. 837–842, Mar. 2015.

[11] M. Song, M. Amelin, X. Wang, and A. Saleem, "Optimized operational

management of an EV sharing community integrated with battery energy storage and PV generation," in *2018 15th International Conference on the European Energy Market (EEM)*, 2018, pp. 1–5.

[12] J. Ostermann and F. Koetter, "Energy-management-as-a-service: Mobility aware energy management for a shared electric vehicle fleet," in *Smart Cities and Green ICT Systems (SMARTGREENS), 2016 5th International Conference on*, 2016, pp. 1–11.

[13] M. Simonov, F. Bertone, and K. Goga, "Global sensitivity analysis workflow support to the EV fleet recharge optimization use case," in *2018 IEEE International Telecommunications Energy Conference (INTELEC)*, 2018, pp. 1–6.

[14] F. Foiadelli, M. Longo, F. Delfino, S. Bracco, D. Spina, and T. Dhaene, "Electric vehicle use in public fleets: The case of the Genoa University," in *2017 International Conference on ENERGY and ENVIRONMENT (CIEM)*, 2017, pp. 490–494.

[15] G. R. Chandra Mouli, M. Kefayati, R. Baldick, and P. Bauer, "Integrated PV Charging of EV Fleet Based on Energy Prices, V2G, and Offer of Reserves," *IEEE Trans. Smart Grid*, vol. 10, no. 2, pp. 1313–1325, Mar. 2019.

[16] C. D. Korkas, S. Baldi, S. Yuan, and E. B. Kosmatopoulos, "An Adaptive Learning-Based Approach for Nearly Optimal Dynamic Charging of Electric Vehicle Fleets," *IEEE Trans. Intell. Transp. Syst.*, vol. 19, no. 7, pp. 2066–2075, Jul. 2018.

[17] R. Carli and M. Dotoli, "A decentralized control strategy for optimal charging of electric vehicle fleets with congestion management," in *2017 IEEE International Conference on Service Operations and Logistics, and Informatics (SOLI)*, 2017, pp. 63–67.

[18] Zihao Jiao, L. Ran, Lei Guan, Xiaohan Wang, and Hongrui Chu, "Fleet management for Electric Vehicles sharing system under uncertain demand," in *2017 International Conference on Service Systems and Service Management*, 2017, pp. 1–6.

[19] R. F. Atallah, C. M. Assi, W. Fawaz, M. H. K. Tushar, and M. J. Khabbaz, "Optimal Supercharge Scheduling of Electric Vehicles: Centralized Versus Decentralized Methods," *IEEE Trans. Veh. Technol.*, vol. 67, no. 9, pp. 7896–7909, Sep. 2018.

[20] S. Liu and A. H. Etemadi, "A Dynamic Stochastic Optimization for Recharging Plug-In Electric Vehicles," *IEEE Trans. Smart Grid*, vol. 9, no. 5, pp. 4154–4161, Sep. 2018.

[21] Maigha and M. L. Crow, "Electric Vehicle Scheduling Considering Co-optimized Customer and System Objectives," *IEEE Trans. Sustain. Energy*, vol. 9, no. 1, pp. 410–419, Jan. 2018.

[22] C. Le Floch, E. C. Kara, and S. Moura, "PDE Modeling and Control of Electric Vehicle Fleets for Ancillary Services: A Discrete Charging Case," *IEEE Trans. Smart Grid*, vol. 9, no. 2, pp. 573–581, Mar. 2018.

[23] Z. Dong, C. Liu, Y. Li, J. Bao, Y. Gu, and T. He, "REC: Predictable Charging Scheduling for Electric Taxi Fleets," in *2017 IEEE Real-Time Systems Symposium (RTSS)*, 2017, pp. 287–296.

[24] A. Kumar, V. Bhalla, and P. Kumar, "Unit commitment in a smart grid with plug-in hybrid electric vehicles — A cost-emission optimization," in *2017 IEEE Transportation Electrification Conference (ITEC-India)*, 2017, pp. 1–6.

[25] S. A. Rahman, Nong Zhang, and Jianguo Zhu, "A comparison on fuel economy and emissions for conventional hybrid electric vehicles and the UTS plug-in hybrid electric vehicle," in *2010 The 2nd International Conference on Computer and Automation Engineering (ICCAE)*, 2010, pp. 20–25.

[26] Y. Ma and J. Wang, "Integrated Power Management and Aftertreatment System Control for Hybrid Electric Vehicles With Road Grade Preview," *IEEE Trans. Veh. Technol.*, vol. 66, no. 12, pp. 10935–10945, Dec. 2017.

[27] J. Liu, Y. Chen, J. Zhan, and F. Shang, "Heuristic Dynamic Programming Based Online Energy Management Strategy for Plug-In Hybrid Electric Vehicles," *IEEE Trans. Veh. Technol.*, vol. 68, no. 5, pp. 4479–4493, May 2019.

[28] H. Yang *et al.*, "Operational Planning of Electric Vehicles for Balancing Wind Power and Load Fluctuations in a Microgrid," *IEEE Trans. Sustain. Energy*, vol. 8, no. 2, pp. 592–604, Apr. 2017.

[29] Z. Darabi, P. Fajri, and M. Ferdowsi, "Intelligent Charge Rate Optimization of PHEVs Incorporating Driver Satisfaction and Grid Constraints," *IEEE Trans. Intell. Transp. Syst.*, vol. 18, no. 5, pp. 1325–1332, May 2017.

[30] G. Ma, M. Ghasemi, and X. Song, "Integrated Powertrain Energy Management and Vehicle Coordination for Multiple Connected Hybrid Electric Vehicles," *IEEE Trans. Veh. Technol.*, vol. 67, no. 4, pp. 2893–2899, Apr. 2018.

[31] T. Chen, B. Zhang, H. Pourbabak, A. Kavousi-Fard, and W. Su, "Optimal Routing and Charging of an Electric Vehicle Fleet for High-Efficiency Dynamic Transit Systems," *IEEE Trans. Smart Grid*, vol. 9, no. 4, pp. 3563–3572, Jul. 2018.

[32] Z. J. Wang and M. Y. Qi, "Formulation of service network design with time requirements to schedule heterogeneous fleet," in *2016 IEEE International Conference on Industrial Engineering and Engineering Management (IEEM)*, 2016, pp. 80–83.

[33] P. Sinruk and Y. Tangmo, "Heterogeneous fleet vehicle routing problem for retail construction material stores," in *2017 4th International Conference on Industrial Engineering and Applications (ICIEA)*, 2017, pp. 234–238.

[34] X. Zeng and J. Wang, "Optimizing the Energy Management Strategy for Plug-In Hybrid Electric Vehicles With Multiple Frequent Routes," *IEEE Trans. Control Syst. Technol.*, vol. 27, no. 1, pp. 394–400, Jan. 2019.

[35] T. Perera, A. Prakash, and T. Srikanthan, "A Hybrid Methodology for Optimal Fleet Management in an Electric Vehicle Based Flexible Bus Service," in *2018 15th International Conference on Control, Automation, Robotics and Vision (ICARCV)*, 2018, pp. 331–336.

[36] F. V. Cerna, M. Pourakbari-Kasmaei, R. A. Romero, and M. J. Rider, "Optimal Delivery Scheduling and Charging of EVs in the Navigation of a City Map," *IEEE Trans. Smart Grid*, vol. 9, no. 5, pp. 4815–4827, Sep. 2018.

[37] F. V. Cerna, M. Pourakbari-Kasmaei, and L. A. Gallego P, "Evaluation of the Performance of HEV Technologies using a MILP Model to Minimize Pollutants Emissions," in *2018 13th IEEE International Conference on Industry Applications (INDUSCON)*, 2018, pp. 446–452.

[38] R. Dan Reid and N. R. Sanders, *Operations Management: An Integrated Approach*, 4th ed. John Wiley & Sons, 2011.

[39] R. G. Schroeder, *Operations Management: Decision Making in the Operations Function*, 4th ed. McGraw-Hill, 1993.

[40] J. L. Gross, J. Yellen, and P. Zhang, *Handbook of Graph Theory*. CRC Press, 2013.

[41] "Data." [Online]. Available: https://drive.google.com/file/d/1e2aaE64xrMr6JKhgkuPBbAuZldkQZn7i/view?usp=sharing.

[42] T. R. Board, Ed., *Highway Capacity Manual*. NW, Washington D. C.: National Academy of Sciences, 2010.

[43] T. R. Board, *HCM 6th Ed.: A Guide for Multimodal Mobility Analysis*. NW, Washington D. C.: National Academy of Sciences, 2016.

[44] L. Elefteriadou, *An Introduction to Traffic Flow Theory*, vol. 84. New York, NY: Springer New York, 2014.

[45] B. T. Kuhn, *Transportation Engineering: A Practical Approach to Highway Design, Traffic Analysis, and Systems Operation*. McGraw Hill Education, 2019.

[46] M. Pourakbari-Kasmaei, M. Lehtonen, M. Fotuhi-Firuzabad, M. Marzband, and J. R. Sanches Mantovani, "Optimal Power Flow Problem Considering Multiple-fuel Options and Disjoint Operating Zones: A Solver-friendly MINLP Model," *Int. J. Electr. Power Energy Syst.*, vol. 113, pp. 45–55, Dec. 2019.

[47] P. S. Iyer, *Operations research*. New Delhi: Tata McGraw-Hill Publishing, 2008.

[48] R. Fourer, D. M. Gay, and B. Kernighan, "Algorithms and Model Formulations in Mathematical Programming," S. W. Wallace, Ed. Berlin, Heidelberg: Springer-Verlag, 1989, pp. 150–151.

[49] "IBM ILOG CPLEX Optimization Studio," 2018. [Online]. Available: https://www.ibm.com/fi-en/marketplace/ibm-ilog-cplex.

Fernando V. Cerna received the B.Sc. degree in Electrical Engineering from the Universidad Nacional del Callao in Lima, Peru, in 2008, the M.Sc and Ph.D degree in electrical engineering from São Paulo State University, Ilha Solteira, Brazil, in 2013 and 2017, respectively, and was a Postdoctoral Fellow during the period 2017-2019 at Londrina State University, Paraná, Brazil. He is a reviewer in several peer-reviewed journals such as IEEE Transactions on Intelligent Transportation System, IEEE Transactions on Sustainable Energy, IEEE Latin America Transactions, Journal of Control, Automation and Electrical Systems and Electric Power System Research.

He is currently an associate professor in the electrical engineering department of the center and science and technology at the Federal University of Roraima, Brazil. His research interests include the development of optimization techniques applied to intelligent energy management, as well as the development of operational strategies for vehicular technologies.

Mahdi Pourakbari-Kasmaei (S'10–M'15) received his Ph.D. degree in electrical engineering, power systems, from the Universidad Estadual Paulista (UNESP), Ilha Solteira, Brazil in 2015. He was a postdoctoral fellow at UNESP and also a visiting researcher at Universidad de Castilla-La Mancha, Spain, for about 15 months. He was a project executive of three practical projects, PI of three academic projects, and also a consultant in an electric power distribution company. Currently, he is a researcher with the Department of Electrical Engineering and Automation, Aalto University, Finland. He is also the Chairman of IEEE PES, IES Finland IE13/PE31/A34/PEL35 Joint Chapter. His research interests include power systems planning, operations, economics, and environmental issues.

Matti Lehtonen was with VTT Energy, Espoo, Finland from 1987 to 2003, and since 1999 has been a professor at the Helsinki University of Technology, nowadays Aalto University, where he is head of Power Systems and High Voltage Engineering. Matti Lehtonen received both his Master's and Licentiate degrees in Electrical Engineering from Helsinki University of Technology, in 1984 and 1989 respectively, and the Doctor of Technology degree from Tampere University of Technology in 1992. The main activities of Dr. Lehtonen include power system planning and asset management, power system protection including earth fault problems, harmonic related issues and applications of information technology in distribution systems.

Javier Contreras (SM'05–F'15) received the B.S. degree in electrical engineering from the University of Zaragoza, Zaragoza, Spain, in 1989, the M.Sc. degree from the University of Southern California, Los Angeles, CA, USA, in 1992, and the Ph.D. degree from the University of California, Berkeley, CA, USA, in 1997.

He is a Professor at the Universidad de Castilla-La Mancha, Ciudad Real, Spain. His research interests include power systems planning, operation, and economics, as well as electricity markets.